



The influence of the annealing mode on stress elimination in a foam glass structure

IRINA GRUSHKO*

Platov South-Russian State Polytechnic University (NPI), Novocherkassk 346428 and Don State Technical University, Rostov-on-Don 344000, Russian Federation

(Received 19 December 2019, revised 24 May, accepted 28 May 2020)

Abstract: The purpose of this work was to establish the influence of features of the annealing mode on the value of residual stresses in the structure of porous inorganic materials using foam glass as an example. A single-stage uniform cooling mode at three different speeds was considered. The study was performed using a mathematical model. The algorithm for analyzing the stress-strain state of the foam glass sample consisted in solving a system of equations by the finite element method. The calculation results are presented in graphic form. The graphics show the changes in stress in the foam glass upon cooling at speeds of 100, 10 and 1 °C min⁻¹. The temperature difference and the viscosity values of the foam glass subsurface and central layers in dependency on different temperatures of the cooling onset are presented. It was concluded that it is necessary to carry out the annealing mode of foam glass in three stages: initial, glass transition step and stabilization step, meaning different cooling rates have to be applied in different stages.

Keywords: Strain; slags; cooling; silicates; finite element method; energy efficiency.

INTRODUCTION

Currently, heat-insulating materials based on dense porous structures, which are used as insulation of facades of buildings and structures for civil and industrial purposes, are becoming more popular.^{1–5} A similar material with a dense porous structure is foam glass, which is characterized by its high thermal insulation ability, mechanical strength, and chemical resistance.^{6–9}

The properties of foam glass depend, for the most part, on the composition of raw materials and the production method.^{10,11}

One of the main technological operations that determines the mechanical strength of foam glass is annealing.^{12,13} However, upon obtaining foam glass that is optimal in all aspects, poor-quality annealing can lead to a sharp increase

* Correspondence E-mail: grushkois@srsru.ru
<https://doi.org/10.2298/JSC191218034G>

in defects in the finished product.¹⁴ At this stage, because of the limited thermal conductivity of the material, changes in the environmental temperature of the foam glass leads to a gradual transfer of heat from one layer of the sample to another. This, in turn, leads to a temperature difference between the outer and inner layers, which cause inner stresses. Those stresses affect the foam glass quality. Thus, it is relevant to study the annealing process and identify patterns of stress formation in foam glass.

Previously,¹⁵ the successful use of mathematical modelling to describe physical and chemical processes at all stages of foam glass production with sufficient accuracy, including at the annealing stage, was established. It seems promising to use the mathematical model proposed by Alekseev and Yashurkaev,^{14,16–18} developed based on the relaxation-kinetic theory of glass transition of Mazurin and Lalykina.^{19,20} Grushko²¹ describes developed software that allows, with minimal time and adequate accuracy, a numerical study of the annealing process to be performed based on the presented mathematical models.

The purpose of this work was to determine the effect of the features of the annealing mode on the value of residual stresses in the structure of porous inorganic materials using foam glass as an example. To achieve this goal, the following objectives have to be solved: identification of the influence of the main parameters of the technological stage of “annealing” (cooling rate and initial annealing rate). Thus, a single-stage uniform cooling mode of foam glass at three speeds was considered: 1 °C min⁻¹ (typical cooling rate for glass products), 10 and 100 °C min⁻¹ (chosen for a more visual demonstration of the processes that occur during annealing of foam glass) and a study of a nonlinear (“three-stage”) annealing mode.

EXPERIMENTAL

The study of the stress-strain state of the foam glass sample during annealing was realized with numerical simulation by solving a system of equations²⁰ by the finite element method in the ANSYS software package,²² according to a previously proposed technique²³ that allows relaxation of the material properties to be taken into account:

$$T_{fi} = T - \int_0^t \exp \left[- \int_{t'}^t \frac{dt''}{\tau_i(t'')} \right] \frac{dT(t')}{dt'} dt' \quad (1)$$

$$T_{fi} = \sum_{i=1}^n g_{it} T_{fi}, \text{ where } \sum_{i=1}^n g_{it} = 1 \quad (2)$$

$$\lg \tau_i = \left(A + \frac{B}{T_{fp} - T_0} - \lg K_i \right) \frac{T_{f\tau}}{T} - \lg \tau_0 \left(\frac{T_{f\tau}}{T} - 1 \right) \quad (3)$$

$$T_{fp} = \sum_{i=1}^n g_{ip} T_{fi}, \text{ where } \sum_{i=1}^n g_{ip} = 1 \quad (4)$$

$$P = P_i(T_{fp}) + \int_{T_{fp}}^T \left(\frac{\partial P}{\partial T'} \right)_{T_{fp}} dT' \quad (5)$$

where T is the temperature, T_f is the structural temperature, t is the time, τ is the relaxation time, g_i are the weight coefficients, n is the number of internal parameters characterizing the structure of the substance, A , B and T_0 are the constants in the Fulcher–Tamman equation; P is property; P_i is the property of a substance in an equilibrium (liquid) state; $K_i = \eta/\tau_i$, here η is the viscosity.

Mathematical modelling of the heat transfer process in the studied object is based on the numerical solution of the initial-boundary-value problem:

$$\rho c = \frac{\partial T}{\partial \tau} = \frac{\partial}{\partial x} \left(\lambda_x \frac{\partial T(x, y, z, \tau)}{\partial x} \right) + \frac{\partial}{\partial y} \left(\lambda_y \frac{\partial T(x, y, z, \tau)}{\partial y} \right) + \frac{\partial}{\partial z} \left(\lambda_z \frac{\partial T(x, y, z, \tau)}{\partial z} \right) \quad (6)$$

where $T(x, y, z, \tau)$ is the desired temperature distribution function; $\lambda_x, \lambda_y, \lambda_z$ are the thermal conductivity coefficients in the direction of the x, y, z axes; ρ is the density; c is the specific heat of the medium.

The stationary heat equation for an isotropic medium has the form:

$$\operatorname{div}(\lambda \operatorname{grad} T) = 0 \quad (7)$$

where T is the desired temperature distribution function; λ is the coefficient of thermal conductivity.

It should be noted that the results of calculating the thermal state are the basis for solving the strength problem.

In this regard, determination of stresses is realized for a system of equations with the following form:²⁴

$$\sigma_{ik} = 2G \left[\varepsilon_{ik} + \frac{\mu}{1+\mu} \frac{S}{2G} \delta_{ik} - \alpha T \delta_{ik} \right] \quad (8)$$

$$\varepsilon_{ik} = \varepsilon_{ki} = \frac{1}{2} \left(\frac{\partial U_k}{\partial x_i} + \frac{\partial U_i}{\partial x_k} \right), i, k=1,2,3 \quad (9)$$

$$\sum \frac{\partial \sigma_{ki}}{\partial x_k} = 0 \quad (10)$$

where σ_{ik} are stresses (σ_{ii} are normal stresses, σ_{ik} ($i \neq k$) are shear stresses; ε_{ik} are distortions; U_i is displacement; $S = \sum \sigma_{ii}$ is the sum of the normal stresses, T is the medium temperature, G is the shear modulus, $2G = E / (1+\mu)$, E is Young's modulus, μ – Poisson's ratio; α – coefficient of thermal expansion and

$$\delta_{ik} = \begin{cases} 1, & i=k \\ 0, & i \neq k \end{cases} \text{ – Kronecker symbol.}$$

The main steps in solving this problem are setting the source data (including the implementation of the solid-state model) and solving and processing the results.

The object of study (Fig. 1) is a sample of foam glass with dimensions of $30 \times 30 \times 30$ mm³, placed on a stand with dimensions of $100 \times 100 \times 3$ mm³, created by powder technology.²⁵

The raw materials were ground in a ball mill with a volume of 5 L to the point of completely passing through a sieve No. 0315, and the batch mixture specific surface area value

was $552 \text{ m}^2 \text{ g}^{-1}$. The batch mixture composition, in mass %: ash and slag waste, 30; crushed glass, 70; borax, 5; anthracite, 5; this composition is 5 over 100 % of the basic components. The estimated chemical composition of the foam glass is given in Table I.

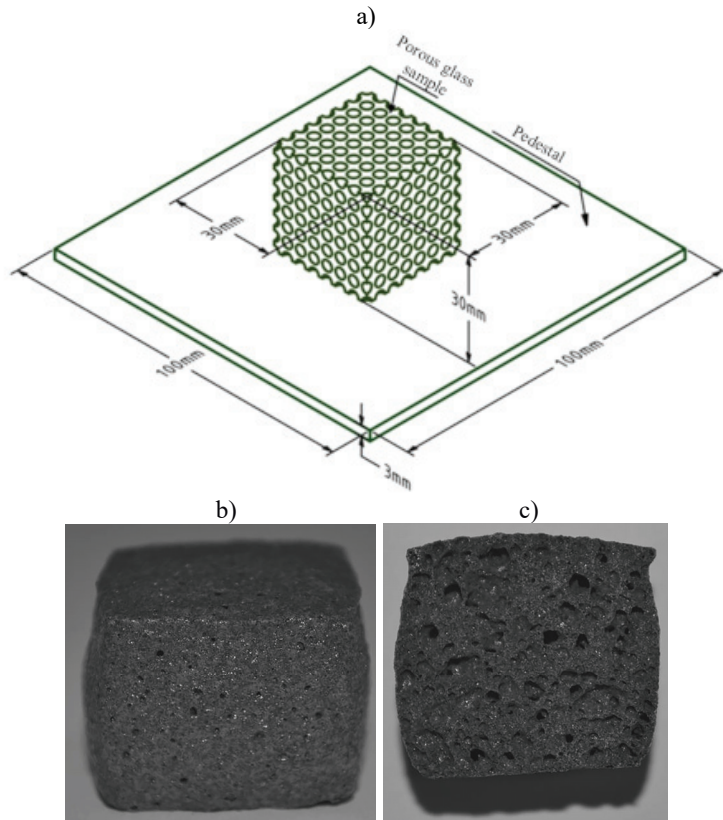


Fig. 1. Object of the study: a) object model view; b) object real view; c) object, longitudinal section.

TABLE I. Composition of the synthesized foam glass

Oxide	Content, mass %	Oxide	Content, mass %
SiO_2	67.33	CaO	7.78
Al_2O_3	6.88	K_2O	1.05
Fe_2O_3	3.73	MgO	0.77
Na_2O	10.71	TiO_2	0.07
P_2O_5	—	SO_3	1.68
PPP	—	Σ	100.00

During heating the ground glass matrix and porous agent batch mixture to 825°C , the gases formed as a result of oxidation or dissociation of the porous agent, the softened glass mass swelled. The sample was foamed and annealed in a muffle furnace with electrical

heaters at a preset temperature–time mode.²⁶ The preset temperature–time mode was as follows: prepared samples were loaded into a cold oven and then heated at $16\text{ }^{\circ}\text{C min}^{-1}$ to $500\text{ }^{\circ}\text{C}$, the temperature for complete combustion of the contained volatile substances. This temperature was maintained for 20 min to ensure an even warming-up of the sample, which has a positive effect on the further process of foaming. Then the temperature was further increased to $825\text{ }^{\circ}\text{C}$, the foaming temperature, and maintained for 20 min. Subsequently, the glass was rapidly cooled to $600\text{ }^{\circ}\text{C}$ to fix the structure of the material. Finally, the sample was cooled to $25\text{ }^{\circ}\text{C}$ at a rate of $2.8\text{ }^{\circ}\text{C min}^{-1}$.

The physical properties of the obtained foam glass sample were determined by building its solid-state model (the visual inspection method was used (Fig. 1) using a ShTs-150 calliper): sample geometry, location and pore size (usually uniformly distributed pore arrangement having an average diameter of 3 mm with a constant gas composition). The construction of a solid model of the foam glass sample was performed using the CAD system software package ANSYS “Space Claim”.

Next, the following physical properties of the obtained sample were determined: thermal conductivity, heat capacity, radiation characteristics, sample geometry, mass, density, Young’s modulus, and Poisson’s ratio.

The calculations used the real thermophysical and radiative properties of carbon dioxide, the foam glass matrix and the steel standard 2Kh18N9T.²⁷⁻³⁰

The values of the thermal conductivity of carbon dioxide at the upper and lower boundary curves, at the critical point and on isobars from 30 to 200 kg cm^{-2} to a temperature of $1000\text{ }^{\circ}\text{C}$ are presented as a function of temperature. For the gas emission process, the ambient temperature and the emissivity of the body were set.

According to the theory of the radiation heat transfer between a radiating and absorbing gas and the surrounding enclosed grey clad, the required emissivity coefficient of the radiative components is given by:

$$\varepsilon_{\text{CO}_2} = f(\rho_{\text{CO}_2}, l, T_g) \quad (11)$$

where ρ_{CO_2} is the partial pressure of the gas mixture and T_g is the temperature of the gas mixture.

For a spherical pore with diameter $D = 3\text{ mm}$, the effective thickness of the gas radiating layer is $l = 1.8\text{ mm}$:

$$l = 0.6D \quad (12)$$

The intensity of gas emission inside the pores of the foam glass decreased in proportion to a decrease in the temperature of the inorganic frame of the foam glass. At the end of the foam glass manufacturing process (at the end of the last production stage), the gas pressure inside the pores was approximately equal to atmospheric pressure. Upon further cooling through the annealing process, the gas pressure decreased by the required amount in certain cells, so that the completely annealed glass exhibited a substantial pressure drop of 33.8 kPa in the cells.³¹ Then, the required emissivity coefficient within the temperature decrease range was 0.01 on average. To estimate the contribution of the radiative compound to the overall temperature distribution, it was assumed that the emissivity coefficient was equal for both the working batch and initial foam glass ($\varepsilon_{\text{gl}} = 0.94$).²⁹

The radiation from the surface of the stand was set in a similar way with its values of the degree of blackness. At the same time, in the block for setting the properties of radiation heat transfer (the variable “Correlations”), the value “Emissions to the environment” was set (“To ambient”).

The thermal conductivity and specific thermal capacity of the foam glass matrix were determined by the laser burst method³² within the temperature range of 25–700 °C using the thermal conductivity measuring system TC-9000H (ULVAC, Japan) at the Common Use Center “Technologies and Materials of National Research University BelSU,” Belgorod, Russia.

TABLE II. Results of the determined thermal conductivity and specific heat of the foam glass

<i>t</i> / °C	<i>T</i> / K	<i>A</i> / cm ² s ⁻¹	<i>C_p</i> / J g ⁻¹ K ⁻¹	<i>k</i> / W cm ⁻¹ K ⁻¹
31.1	304.1	0.00592	0.87296	0.00757
101.1	374.1	0.00567	0.85875	0.00714
200.1	473.1	0.00538	0.93964	0.0074
300.4	573.4	0.00528	1.18179	0.00913
399.7	672.7	0.0052	1.20185	0.00914
499.3	772.3	0.00553	1.19574	0.00968
599.3	872.3	0.00572	1.37081	0.01149
699.4	972.4	0.00517	1.62584	0.0123

The value of thermal conductivity λ was calculated by the formula:

$$\lambda = \alpha C_p \rho_k \quad (13)$$

where $\rho_k = 146 \text{ kg m}^{-3}$ is the sample density.

The density of the sample was calculated by the formula EN 1602:1996 “Thermal insulating products for building applications – Determination of apparent density”:

$$\rho_k = \frac{m}{V} \quad (14)$$

where m is the mass of material, kg; V is the volume of the material, including pores and voids, m³, and $\rho_k = 146 \text{ kg m}^{-3}$.

To determine Young's modulus, tests of foam glass samples were carried out according to the procedure presented in EN 13167:2012 “Thermal insulation for building – Factory made cellular glass (CG) products – Specification” was applied. The essence was to measure the value of the compressive forces necessary to destroy the sample under appropriate test conditions.

Cubic samples with sizes of 30×30×30 mm³ were mounted in a hydraulic press so that the compressive force was directed along the vertical axis of the sample. Additionally, one 250 UW strain gauge with a vertical axis (longitudinal strain gauge) and one gauge with a horizontal axis (transverse strain gauge) were glued on the sides of the cross-section of the foam glass sample, each of which was connected via a half-bridge circuit to a separate channel of the UTS-1 strain gauge station. The process of loading the sample had an initial load of 500 N in increments of 250 N until the visual destruction of the sample. In addition, by sequentially switching the corresponding channels of the strain gauge station, the readings of each of the strain gauges were taken.

The sample pressure, σ , Pa, is determined by the formula:

$$\sigma = \frac{P}{lb} \quad (15)$$

where P is the applied load, N; l is the sample length, m, and b is the sample width, m.

The relative longitudinal strain, $\varepsilon_{\text{long}}$, was determined by the formula:

$$\varepsilon_{\text{long}} = \frac{\Delta l}{l_0} \quad (16)$$

where Δl is the defined elongation and l_0 is the initial sample length.

The relative transverse strain, $\varepsilon_{\text{transv}}$, was determined by the formula:

$$\varepsilon_{\text{transv}} = \frac{\Delta d}{d_0} \quad (17)$$

where Δd is the transverse sample size and d_0 is the initial sample size.

When the force reached 2250 N, the pressure on the sample created a stress exceeding the shear stress, and the material entered the stage of plastic deformation. At a moment corresponding to a force of 2500 N, destruction of the material occurred.

In accordance with Hooke's Law, the elastic modulus of the sample material was determined:

$$E = \frac{\sigma}{\varepsilon} \quad (18)$$

therefore, $\sigma = 2.6 \text{ MPa}$, $\varepsilon = 0.002070$ and $E = 1256 \text{ MPa}$.

According to the results of tensometric measurements, the dependence of the transverse strain on the longitudinal strain under compression was obtained.

The experimental results were approximated by a straight line using the least squares method. The result of the standard error was 1.07×10^{-8} .

The determined value of the Poisson's ratio was:

$$\mu = \frac{\varepsilon_{\text{transv}}}{\varepsilon_{\text{long}}} = \frac{0.0004554}{0.002070} = 0.22 \quad (19)$$

where μ is the Poisson's ratio, $\varepsilon_{\text{transv}} = 0.0004554$ is the lateral relative deformation and $\varepsilon_{\text{long}} = 0.002070$ is the longitudinal relative deformation.

The obtained values of the physical properties of the matrix material of the foam glass sample using the module "Engineering Data" with the additional shell interface "Workbench" used descriptions of the properties of materials, and input parameters of the mathematical models are listed in the created mathematical model.

To solve unsteady heat conduction problems, a transient thermal module with the following boundary conditions was used.

The boundary conditions were specified in the form of temperature $T = f(\text{time})$ on the outer surface of the foam glass sample in the study. The calculation was performed under the assumption that the temperature of the surface of the sample changed according to a given mode (the physical possibility of the claimed mode could be achieved due to the significant convective heat transfer of heat from the foam glass surface, providing a given cooling rate of the sample (the temperature of the gaseous medium around the sample should be much lower than its surface temperature)).

The maximum time step value was determined to be 10 s according to the literature.³³

RESULTS AND DISCUSSION

The stress changes in the sample during cooling starting from 600 °C at different speeds: a) 100, b) 10 and c) 1 °C min⁻¹ are shown in Fig S-1 of the

Supplementary material to this paper. As can be seen from Fig. S-1, the stress increase occurs in two stages.

In the initial period of uniform cooling, there is a rapid increase in the temperature difference between the centre (Fig. S-2 of the Supplementary material) and the surface of the object in question, which leads to an increase in temperature stresses and their subsequent decrease due to an intense relaxation process.³⁴ In the second stage of annealing, which occurs in the glass transition region (the range of the decimal logarithm of the viscosity of the foam glass is 10–16 Pa·s, Fig. S-3 of the Supplementary material), the stress values increase, the rate of change of which becomes minimal, which leads to the appearance of residual stresses. It should be noted that the available stress effects are inversely proportional to the rate of annealing.

The temperature difference between the subsurface and central layers of a sample depending on various temperatures of cooling onset are shown in Fig. S-2 of the Supplementary material. The cooling rate was set as a constant, and its value was $1.5 \text{ }^{\circ}\text{C min}^{-1}$ regardless of the initial annealing temperature.

With uniform cooling, the stresses in the subsurface layers of the foam glass are compression stresses (Fig. S-1), since at the beginning of the annealing process, the temperatures of the subsurface layers were lower than the temperatures of its central layer (Fig. S-2), while the free dimensions of the surface layers decreased to a greater extent than the dimensions of the central layer. However, in the glass transition interval, the free sizes of the inner layers decrease to a greater extent than the free sizes of the outer layers. As a result of these processes, the residual stresses in the subsurface layers are compression stresses, and in the central layers, tensile stresses.

The viscosity values of the subsurface and central layers in dependence on different temperatures of cooling onset are shown in Fig. S-3. The cooling rate is set as a constant, and its value was $1.5 \text{ }^{\circ}\text{C min}^{-1}$ regardless of the initial annealing temperature.

The stresses occurring in the foam glass during annealing with different initial temperatures are presented in Figure S-4 of the Supplementary material. Evidently, an increase in the initial annealing temperature (while maintaining a constant rate of the cooling process) practically does not change the value of the residual stresses and retains the shape of the curve.

Thus, the heat treatment of foam glass during the annealing process has a different effect on the formation of its stress-strain state, which allows us to conclude that different values of the rate of temperature change at different stages are necessary. The foam glass annealing mode is nonlinear and it is advisable to divide it into three stages: initial (stage 1), glass transition (stage 2) and stabilization stage (stage 3), and the cooling rates in the first and third stages are much higher than in

the second stage, the temperature range of which is the critical cooling interval.^{14,16–18} As a rule, the cooling rates at different stages differ several times.¹³

Consideration of a three-stage annealing mode. The dependence of stress, viscosity and temperature of the subsurface and central layers on time are shown in Figs. S-5–S-7 of the Supplementary material.

In the temperature range of 600 °C, an increase in stresses is formed, associated with the beginning of the glass transition interval, the viscosity of the layers is relatively small, the significant stresses that arise begin to relax initially at a high speed, then gradually reduce it. The cooling rate again increases from a temperature of 460 °C. In this case, the temperature difference between the centre and the surface of the foam glass increases again, however, these changes are significantly slower than after a sharp decrease in speed. Moreover, the total value of the effect in this case is more significant than in the case of a decrease in the cooling rate, as a consequence of 3–4 orders of magnitude higher viscosity at 460 °C than viscosity at 600 °C, so stress relaxation is practically absent. Thus, stress relaxation in the second cooling stage affects residual stresses favourably.

CONCLUSIONS

Analysis of the information presented allows the following conclusions to be drawn:

1) with uniform cooling, the growth of stresses occurs in two stages, the value of which is proportional to the rate of annealing: the first stage is determined by temperature stresses and their subsequent decreases due to the intense relaxation process; the second stage corresponds to the glass transition area (the range when the decimal logarithm of the viscosity of the foam glass is 10–16 Pa s), where there is a new increase in stresses, the rate of change of which becomes minimal, and then leads to the appearance of residual stresses;

2) the residual stresses in the subsurface layers are compression stresses, and in the central layers tensile stresses, due to the fact that at the beginning of annealing, the temperature of the subsurface layers was lower than that of its central layer, while the free dimensions of the surface layers decrease to a greater extent than the dimensions of the central layer, but then, in the glass transition interval, the free sizes of the inner layers decrease to a greater extent than the free sizes of the outer layers;

3) the heat treatment of foam glass during the annealing process has a different effect on the formation of its stress–strain state, which allows us to conclude that different values of the rate of temperature change at different stages are necessary. It is advisable to divide the foam glass annealing mode into three stages: initial (step 1), glass transition (step 2) and stabilization step (step 3);

4) stress relaxation at the glass transition stage favourably affects the residual stresses because the viscosity values at a temperature of 460 °C are 3–4

orders of magnitude higher than the corresponding values at a temperature of 600 °C and stress relaxation is practically absent.

SUPPLEMENTARY MATERIAL

Additional data are available electronically at the pages of journal website: <https://www.shd-pub.org.rs/index.php/JSCS/index>, or from the corresponding author on request.

ИЗВОД

УТИЦАЈ РЕЖИМА ОДГРЕВАЊА НА УКЛАЊАЊЕ НАПРЕЗАЊА У ПЕНАСТОМ СТАКЛУ

IRINA GRUSHKO

Platov South-Russian State Polytechnic University (NPI), Novocherkassk 346428 и Don State Technical University, Rostov-on-Don 344000, Russian Federation

Циљ овог рада је дефинисање утицаја начина одгревања на заостала напрезања у структури порозних неорганских материјала, на примеру пенастог стакла. Разматран је утицај три брзине током једностепеног униформног режима хлађења. Коришћењем математичког модела који је добијен методом коначних елемената анализирана су настала напрезања у стаклу. Графички су приказане зависности напрезања од времена при брзинама хлађења 100, 10 и 1 °C min⁻¹. Приказане су разлике температуре и вискозности потповршинског и централног слоја од времена, за различите почетне температуре одгревања. Закључено је да режим одгревања мора да се изводи у три корака различитих брзина: почетни, прелазни и стабилизациони.

(Примљено 19. децембра 2019, ревидирано 24. маја, прихваћено 28. маја 2020)

REFERENCES

1. K. S. Ivanov, *Mag. Civ. Eng.* **5** (2019) 52 (<https://dx.doi.org/10.18720/MCE.89.5>)
2. Y. V. Selivanov, A. D. Shiltina, V. M. Selivanov, Y. V. Loginova, N. N. Korolkova, *Mag. Civ. Eng.* **3** (2012) 35 (<https://dx.doi.org/10.5862/MCE.29.4>)
3. B. S. Semukhin, O. V. Kazmina, A. Y. Volkova, V. I. Suslyayev, *Rus. Phys. J.* **12** (2017) 2130 (<https://dx.doi.org/10.1007/s11182-017-1024-8>)
4. L. Lakov, B. Jivov, M. Aleksandrova, Y. Ivanova, K. Toncheva, *J. Chem. Tech. Met.* **6** (2018) 1081 (https://dl.uctm.edu/journal/node/j2018-6/8_17-204_p_1081-1086.pdf)
5. S. Schiavoni, F. D'Alessandro, F. Bianchi, F. Asdrubali, *Renew. Sust. Energy Rev.* **62** (2016) 988 (<https://dx.doi.org/10.1016/j.rser.2016.05.045>)
6. J. Zach, M. Sedlmajer, J. Bubenik, M. Drdlova, *IOP Conf. Ser.: Mater. Sci. Eng.* **583** (2019) 012016 (<https://dx.doi.org/10.1088/1757-899X/583/1/012016>)
7. Z. Qin, G. Li, Y. Tian, Y. Ma, P. Shen, *Mater.* **12** (2018) 54 (<https://dx.doi.org/10.3390/ma12010054>)
8. C. Xi, F. Zheng, J. Xu, W. Yang, Y. Peng, Y. Li, P. Li, Q. Zhen, S. Bashir, J.L. Liu, *Constr. Build. Mater.* **190** (2018) 896 (<https://dx.doi.org/10.1016/j.conbuildmat.2018.09.170>)
9. O. V. Puchka, V. S. Lesovik, N. I. Minko, S. S. Vaysera, M. A. Frolova, *Res. J. Appl. Sci.* **10** (2014) 674 (<https://medwelljournals.com/abstract/?doi=rjasci.2014.674.679>)
10. O. V. Kazmina, S. N. Volland, M. A. Dushkina, *IOP Conf. Ser.: Mater. Sci. Eng.* **64** (2014) 012015 (<https://dx.doi.org/10.1088/1757-899X/64/1/012015>)
11. R. R. Petersen, J. König, Y. Yue, *J. Non-Cryst. Solids* **425** (2015) 74 (<https://dx.doi.org/10.1016/j.jnoncrysol.2015.05.030>)
12. I. I. Kitajgorodskiy, *Penosteklo*, Strojizdat, Moscow, 1958
13. B. K. Demidovich, *Penosteklo*, Nauka i Technika, Minsk, 1975

14. A. I. Shutov, L. I. Yashurkaeva, S. V. Alekseev, T. V. Yashurkaev, *Glass Ceram.* **64** (2007) 397 (<https://dx.doi.org/10.1007/s10717-007-0099-z>)
15. I. S. Grushko, *Glass Ceram.* **73** (2017) 355 (<https://dx.doi.org/10.1007/s10717-017-9888-1>)
16. A. I. Shutov, S. V. Alekseev, T. V. Yashurkaev, *Glass Ceram.* **63** (2006) 213 (<https://dx.doi.org/10.1007/s10717-006-0082-0>)
17. A. I. Shutov, L. I. Yashurkaeva, S. V. Alekseev, T. V. Yashurkaev, *Glass Ceram.* **64** (2007) 297 (<https://dx.doi.org/10.1007/s10717-007-0074-8>)
18. A. I. Shutov, S. V. Alekseev, T. V. Yashurkaev, *Tech. Technol. Silic.* **13** (2006) 14 (<https://elibrary.ru/item.asp?id=12909525>)
19. O. V. Mazurin, *Steklovanije & Stabilizacija Neorganicheskikh Stekol*, Nauka, Leningrad, 1978
20. O. V. Mazurin, *Steklovanije*, Nauka, Leningrad, 1986
21. I. S. Grushko, *Izv. Vish. Uch. Zav. Sev.-Kav. Reg. Ser.: Tech. Sci.* **2** (2018) 90 (<https://dx.doi.org/10.17213/0321-2653-2018-2-90-95>)
22. N. N. Fedorova, S. A., Valger, M. N. Danilov, Yu. V. Zaharova, *Osnovi raboti v Ansys 17*, DMK Press, Moscow, 2017
23. O. Yu. Smetannikov, N. A. Trufanov, *Vich. Mech. Splosh. Sred.* **1** (2008) 92.
24. E. Melan, G. Parkus, *Termouprugie naprjazhenija, vizvannie stacionarnimi temperaturnimi poljami*, Fizatgiz, Moscow, 1958
25. I. Grushko, in *13th International Scientific-Technical Conference on Dynamic of Technical Systems*, 2017, Rostov-on-Don, Russia, *XIII International Scientific-Technical Conference "Dynamic of Technical Systems" (DTS-2017)*, MATEC Web Conf., EDP Sciences, Les Ulis, France, 2017, Abstract No. 03006 (<https://dx.doi.org/10.1051/matecconf/201713203006>)
26. I. S. Grushko, *IOP Conf. Ser.: Mater. Sci. Eng.* **389** (2018) 012001 (<https://dx.doi.org/10.1088/1757-899X/389/1/012001>)
27. GS SSD 101-86: *Diocsid ugleroda. Koefficienti vjazkosti, teploprovodnosti i chislo Prandtlja razrezhennogo gaza v diapazone temperatur 150–2000 K / Tablici spravochnih dannih*, 1986
28. N. V. Cederberg, *Teploprovodnost gazov i zhidkostej*, Gosenergoizdat, Moscow, 1963
29. L. N. Latyev, V. A. Petrov, V. Ya. Chehovskij, E. N. Shestakov, *Izluchatelniye svojstva tverdih materialov: spravochnik*, Energija, Moscow, 1974
30. A. Minsar, *Teploprovodnost tverdih tel, zhidkostej, gazov i ih kompozicij*, Mir, Moscow, 1968
31. F. Shill, *Penosteklo*, Izdatelstvo literaturi po stroitelstvu, Moscow, 1965
32. V. G. Baranov, A. V. Tenishev, A. V. Lunev, S. A. Pokrovskij, A. V. Hlunov, *Jad. Fiz. Inzhin.* **4** (2011) 291
33. O. V. Mazurin, Yu. K. Starcev, R. Ya. Hodakovskaja, *Relaksacionnaja teorija otzhiga stekla i raschet na ee osnovne rezhimov otzhiga*. Uchebnoe posobie. MHTI named by D.I. Mendeleev, Moscow, 1987
34. O. V. Mazurin, Yu. L. Belousov, *Otzhil I Zakalka Stekla*, MISI&BTISM, Moscow, 1984.